

PIV as a Novel Full-Scale Measurement Technique in Cavitation Research

Andre Kleinwächter¹, Katrin Hellwig-Rieck², Eric Ebert¹, Robert Kostbade¹,
Hans-Jürgen Heinke², Nils A. Damaschke¹

1: Dept. of Optoelectronics and Photonic Systems, University of Rostock, Germany

2: Dept. of Propeller and Cavitation, Potsdam Model Basin (SVA), Potsdam, Germany

ABSTRACT

In order to validate calculation algorithms for full-scale wake fields measured data are highly desired. For this reason a robust and not too complex PIV-measurement system had been developed, tested and used for velocity measurements on board of the ConRo-ship "Amandine".

The comparison of the measured and calculated total velocity components in front of the propeller of the ConRo-ship "Amandine" shows in general a higher inflow speed in the wake peak than calculated. The influence of the propeller on the local inflow velocities was measured and calculated with a good correlation.

The full-scale measurements and calculations had been used for the validation of the cavitation test procedure in the cavitation tunnel K15A of the SVA Potsdam. The simulation of the calculated nominal wake field for the Reynolds number of the ship using a dummy model and additional wire grids leads to a total propeller inflow field similar to the full-scale conditions. Cavitation observations and measurements of the pressure fluctuations are discussed in comparison to full-scale data.

Keywords

Propulsion, propeller, wake field, tip vortex cavitation, pressure fluctuation, full-scale measurement, PIV.

1 INTRODUCTION

Important aspects of the ship and propeller design are the propulsion efficiency and the vibration level in the aft ship. The propeller induced pressure fluctuations as well as the underwater noise are mainly influenced by the cavitation behavior of the propeller. The reliable cavitation prediction in the propeller design process is therefore essential.

The distribution of the wake fraction components is very important for the cavitation dynamic during each revolution of the propeller. The measurement of the nominal wake field in model scale and the use of scaled wake fields is a part of the propeller design process. Viscous flow calculation methods are now able to calculate the flow

around the ship without and with working propeller for the Reynolds numbers of the model and of the ship. As a consequence calculated full-scale wake field data are used for the propeller design and also for cavitation tests, ITTC (2011).

The validation of the results of the cavitation and pressure fluctuation calculations demands model and full-scale measurements. Especially measurements of the propeller inflow in full-scale are missing for the validation of propeller calculations, ITTC (1999). For this reason it is highly desired to establish a robust measurement technique to record reliable full-scale wake field data with reasonable effort.

The joint R&D-project KonKav II was dedicated to evaluate the influence of the scale (Reynolds number) on the propeller inflow and the cavitation behavior of the propeller. KonKav II was supported by the Federal Ministry of Economic Affairs and Energy (BMWi) and completed in 2013. The Hamburg Ship Model Basin (HSVA), Potsdam Model Basin (SVA), Technical University of Hamburg-Harburg (TUHH), Flensburger Schiffbau-Gesellschaft mbH & Co. KG (FSG) and the University of Rostock (UHRo) were involved in the project.

The total inflow field of the working propeller at a ship was measured in connection with cavitation observations and pressure fluctuation measurements. To record the wake fraction distribution PIV-technique (Particle Image Velocity) was adapted to the rough measurement environment inside a ship for the first time, Kleinwächter et al. (2014). This paper discussed the novel PIV full-scale measurement system with the focus on its applicability in relation to the former used LDV-technique (Laser Doppler Velocimetry), Kux et al. (1982) or Kuiper et al. (2002), and the requirements inside the ship.

Furthermore the use of the data for the validation of CFD-calculations and cavitation test procedures will be shown.

2 SUBJECT OF STUDY

The ConRo-ship ConRo220 “Amandine” (Figure 1) was built by FSG and had been selected for full-scale measurements, viscous flow calculations and model tests. The main data of the ConRo-ship are summarised in Table 1. The Table 2 presents the main data of the propeller.

Table 1: Main dimensions of the ship.

Length	L_{PP}	[m]	186.22
Breadth	B	[m]	30.00
Draught aft	T_a	[m]	6.65
Draught fore	T_f	[m]	6.32



Figure 1: ConRo-ship “Amandine”.¹

Table 2: Main dimensions of the propeller.

Propeller type			CPP
Diameter	D	[m]	5.80
Area ratio	A_E/A_0	[-]	0.65
Number of blades	Z	[-]	4

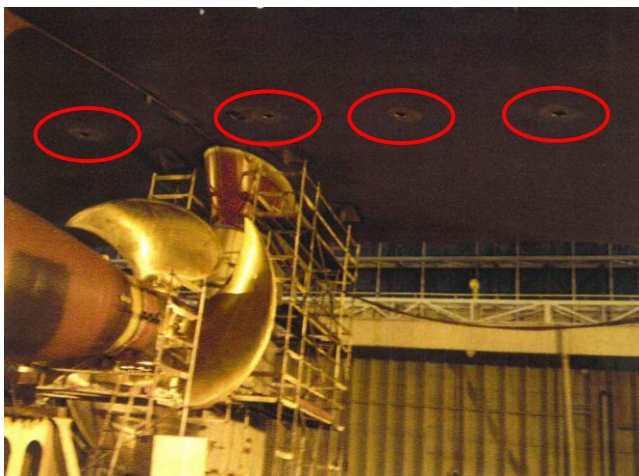


Figure 2: Portholes in the propeller plane of the ConRo-ship “Amandine”.

The ship had been equipped by FSG with four portholes in the propeller plane for cavitation observations and with pressure pick-ups for the measurement of the propeller induced pressure fluctuations (Figure 2).

3 ADAPTATION OF THE PIV-TECHNIQUE FOR FULL-SCALE VELOCITY MEASUREMENTS

The main concepts of the used measuring system are described in detail by Kleinwächter et al. (2014). The measurement principle is based on a double illumination and imaging of the flow at defined time intervals. The subsequent velocity calculation is based on a correlation estimation of the captured particle structures, Raffel et al. (2007). A schematic configuration of the main setup components to conduct PIV-measurements on board of the ConRo-ship “Amandine” is shown in Figure 3.

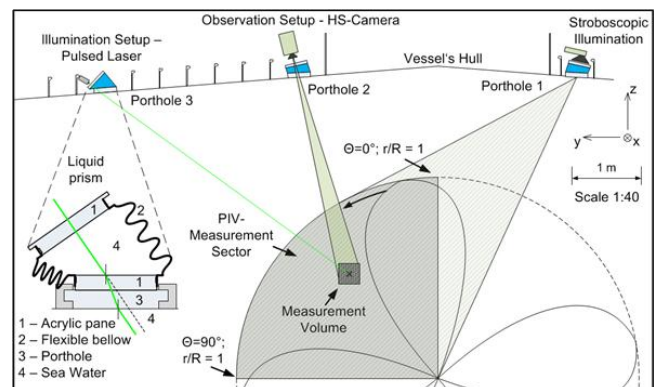


Figure 3: Schematic measurement setup / optical access / measurement sector.

In order to characterize the entire measuring area spatially resolved, both the observation and illumination setup was pivoted. Since the portholes were arranged almost in the propeller plane, the measurement system had to be rotated about the y-axis too in order to measure the flow velocities in front of the propeller (Figure 5).



Figure 4: Measurement setup inside the steering gear compartment.

¹ www.marinetraffic.com

Precise and vibration-resistant motorized linear and rotation stages mounted on an X95-profile system were used for an automatic definition of each single measurement volume (MV). The alignment of the complete setup was accomplished by a cross line leveling instrument, which defines a Cartesian coordinate system. The waterlines inside the vessel were used as reference edges. Figure 4 depicts the PIV-measurement system, stiffly clamped on vessel's H-profiles. Liquid water filled prisms, shown in the left of Figure 3 ensure constant and minimal aberrations in a defined optical path despite the necessary rotations.

The laser pulses and picture capturing were synchronized and triggered by the shaft signal. For that purpose the absolute 0°-position had to be identified by means of stroboscopic illumination of the propeller over porthole 1 (Figure 3). The shaft triggered measurements were performed at four discrete propeller angles ($\theta = 0^\circ, 22.5^\circ, 45^\circ$ and 67.5°) to identify the strong propeller impact on the velocities due to the close distance to the measurement plane.

Since PIV is an optical measurement system the distortions of the recorded pictures have to be equalized. It was not feasible to mount a calibration target in the region of interest neither during the voyage nor at the harbor. By inserting and capturing two parallel laser beams with a defined distance into each measurement volume the spherical and perspective aberrations became obvious. The strong astigmatism due to the oblique position of the liquid prisms in the optical path has no significance for the analysis algorithms. A calibration matrix was generated and applied on the velocity records. The known distance between the rays determines the necessary spatial length dimension for the velocity calculation.

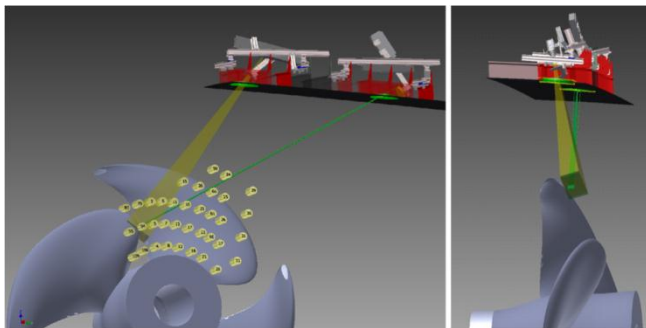


Figure 5: Simulated measurement equipment, ship's hull, measurement volumes and propeller.

For a subsequent comparison with simulation data the recorded velocity field has to be transformed from picture into ship coordinates. The calculations include two rotations with exactly the angles used for defining each single measurement volume.

3.1 Capabilities, Limitations and further Developments of the PIV-System

Compared with previously executed LDV-measurements (Laser Doppler Velocity) the PIV-measurement system convinces with the following advantages:

- Rugged system against vibrations, grease and high humidity due to a relatively uncomplicated modular and encapsulated setup
- Large angular measuring range at nearly constant recording conditions
- Smaller measurement installation and data analysis effort
- High statistical confidence because of a higher data rate (D), leading additionally to shorter measurement times

In previous full-scale measurements, e.g. presented in Kux (1982), a typical data rate in the near field (around 1 m) was about ten measurements per second. In a distance of 4 to 5 m the value even decreased to a few measurements per minute (left of Figure 6). The depicted data rate was also normalized to the local mean wake fraction (w) since D depends on w in LDV-measurements.

With PIV in contrary a mean secure data rate in an observation distance of 3.5 m was about 350 velocity samples per second (right of Figure 6). Since the data rate depends not only on the observation distance but also on the laser energy attenuation on the observed volume, the data is depicted over the sum of the laser beam distance and the observation distance to the measurement volume.

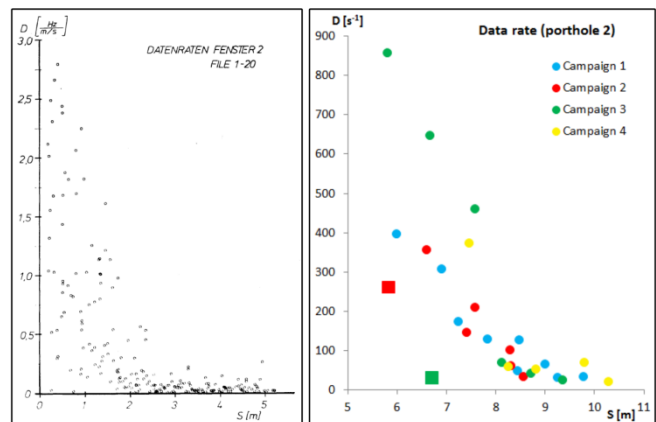


Figure 6: LDV data rate referred to the distance of the measurement volume (left), Kux (1982); PIV data rate over the whole optical path.

The size of a mean detection volume (0.04 m^2) and a spatial averaging over the imaged region (transition from 2D2C to 0D2C) are the reasons for that huge difference in the data rate of both techniques. Nearly 60 valid vectors in a double frame lead at a frame rate of about 7 Hz (propeller blade frequency) to 400 samples per second. After an overall measurement time of 50s 20000 velocity samples are recorded for a reliable statistics. The data rate can even be

exceeded when the measurements are triggered by the maximum repetition rate of the used laser (15 Hz).

Both methods have an exponential decay of the data rate in common due to the scattering of light on particles in water. The PIV data rate also drops since the image section decreases for higher distances at a unique detection volume, provided that lenses with a fixed focal length are used.

Figure 6 also depicts the dependency of the data rate from the visibility in water, which is worse in the purple highlighted region (Figure 7). In Campaign 2 and 3 the data points marked by a square (Figure 6) were recorded first and last respectively in the campaigns. Despite the small distances to the measuring volume, the data rate is significantly worse than at other points with comparable distances. However, a minimum number of particles is necessary for a statistically safe velocity determination. The data rate increases at a constant distance as the size of the interrogation area can be reduced. Further features of the measurement system are:

- No restrictions concerning the ship velocity range
- Vibrations onboard are neglectable due to their ten times lower frequencies compared with the double pulse rate of image acquisition
- Parallel recording of vibrations and ship movement (roll, pitch) to correlate the velocity measurements
- Validated measurement system: reference measurements have been executed in the towing tank of SVA (relative systematic velocity error is below $\Delta u/u = 5\%$)

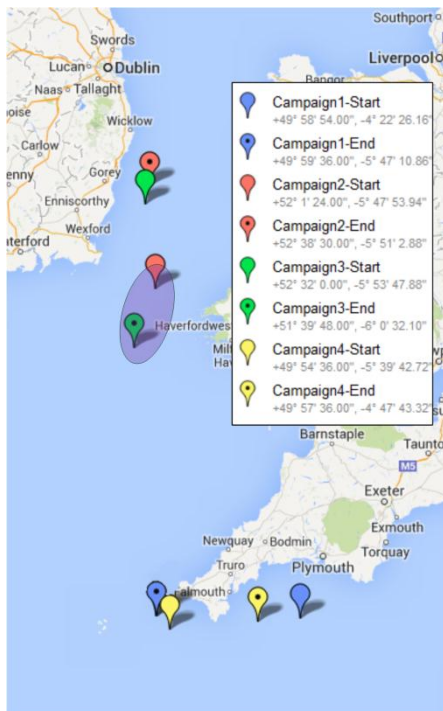


Figure 7: Four measurement campaigns during a round trip from Rotterdam to Dublin and back, defined by the visibility in water.

- Calibration of positioning the system over a mounting hole on the stern tube for the rope guard (positioning inaccuracy between 1 and 3 cm, depending on the distance)
- Repeatability of positioning below 2 mm in a distance of 4 m (mainly determined by the bidirectional repeatability of the rotation axis): separate recording of calibration and velocity videos or repositioning for single spots possible
- Shaft triggered and synchronized measurements (FPGA) for phase-resolved velocity data with a delay of one propeller revolution; highly needed to identify the propeller induced velocities

The measurement system at the current state is capable to record 0D2C-PIV data. The short measurement time on the voyages, the high development effort for 3C and the fact that the error of the wake fraction after transforming the picture data in ship coordinates due to the missing w-component is below 1% were the reasons for shifting the 0D3C – PIV development in a subsequent project.

The biggest constraint is the necessity for good visibility in sea water. Figure 6 proves that measurements above 4 m and 6 m (MV95) for the observation and illumination distance respectively are feasible (Figure 8). Even a data rate of 23 samples leads after only 10 min to about 14000 velocity vectors.

The second restriction results out of the frame construction. Figure 8 visualizes the maximum angles for PIV at the moment. The porthole dimensions prevent higher illumination angles. Observation angles are limited by the reduced aperture and the therefore lower light intensity. The most interesting area around $\theta = 0^\circ$; $r/R = 1$ however couldn't be observed because of the unfavorable frame construction around the portholes. The red circles in Figure 8 and the pictures in Figure 9 depict the collision points.

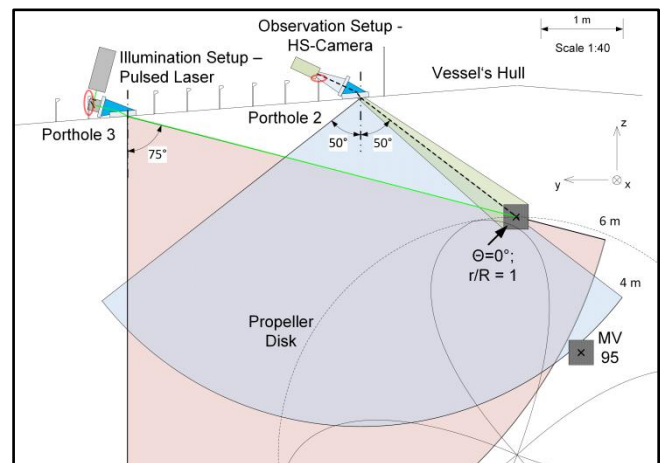


Figure 8: Measurement sector beneath “Amandine”.



Figure 9: Tilting limitations due to ship's frame construction at porthole 2 (right); disturbing toe bracket for rotation around Y (left).

Another constraint is the restricted time on a measurement voyage. Parameters like data rate, the amount of measurement volumes and discrete propeller angles and the possibility to obtain constant propulsion, course and weather conditions have to be weighed against each other. Additionally the maximum usable laser energy is limited by the porthole panes and was adapted to exclude destructions.

The weakest point of the system at the moment is the vulnerability of the optical elements with regard to the harsh environmental conditions (grease, high humidity, etc.) in the steering gear compartment of the ship. In order to avoid pollutions a laminar flow around all beam deflecting elements will be retrofitted. Further developments are:

- Possibility to record 0D3C-velocity data based on a setup exchange to gain a second observation direction (Stereoscopic PIV)
- Extension of the adapters in order to mount the system on all possible H-profiles
- Redesign of the liquid prisms for a higher dynamic in positioning the measurement equipment
- Development of a tube similar to the Boroskop, presented by Carlton (2012) for the illumination setup to allow for angles larger than 75° in order to illuminate ship's boundary layers
- Expanding the laser to a laser light sheet before the porthole pane instead of using a single cylindrical lens to increase the energy transmission and obtain higher data rates and larger measurement distances

3.2 Requirements for the Ship and the Route

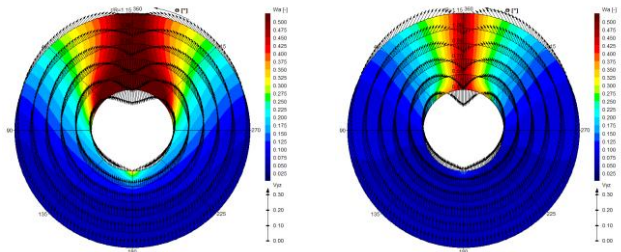
Besides a good visibility in sea water two portholes are at least necessary to observe the wake field. Most important is the choice of the porthole positions. At "Amandine" a segregated ballast tank prevented a porthole positioning far away from the propeller, to measure a wake with minimal propeller induced velocities. The porthole surroundings should allow for wide tilting angles (Figure 8). The assurance of approximately constant flow, weather and propulsion parameters is mandatory to correlate the measured data with simulations. This holds especially true for 3C-measurements, which have to be executed sequentially. Furthermore power supply sockets and a BNC-

cable from the engine room to the portholes have to be provided if shaft triggered measurements are desired.

4 FULL-SCALE MEASUREMENTS AND CFD-CALCULATIONS FOR DETERMINATION OF THE PROPELLER INFLOW FIELD

4.1 Nominal Wake Field

Figure 10 presents the calculated nominal wake field (ship without propeller and rudder) of the ConRo-ship "Amandine" for the model and the full-scale Reynolds numbers.



model scale, $Re_M = 1.12 \cdot 10^7$ **full-scale, $Re_S = 1.33 \cdot 10^9$**
Figure 10: Calculated nominal wake fields.

The comparison of both wake fields shows the typical scale effect on the propeller inflow of single screw ships, ITTC (2011). The wake peak at the full-scale Reynolds number is distinctly smaller than in model scale. A validation of the CFD calculation for the full-scale Reynolds number is possible only indirectly over measurements of the total wake at a ship or the analysis of cavitation observations and pressure fluctuation measurements.

4.2 Total Wake Field

Measurements of the total velocity components in front of the propeller of the ConRo-ship "Amandine" had been carried out on the voyage from Rotterdam to Dublin and back, as shown in Figure 7. The measurement points in the propeller coordinate system are located on non-dimensional radii, as listed in Table 3 and shown in Figure 11.

Table 3: Velocity measurement points

$r/R = 0.55$		$r/R = 0.70$		$r/R = 0.85$		$r/R = 1.00$	
MV	θ_s [°]						
95	333.5	80	338.5				
94	343.1	79	346.6				
3	351.8	2	353.6				
7	0.0	6	0.0				
12	8.2	11	6.4	15	11.0	50	22.4
17	17.0	16	13.5	20	18.3	24	27.7
22	26.5	21	21.5	66	24.8	29	38.7
96	33.1	81	27.9	25	30.4		
27	40.5	26	34.3	30	42.6		
32	56.6	31	47.9				

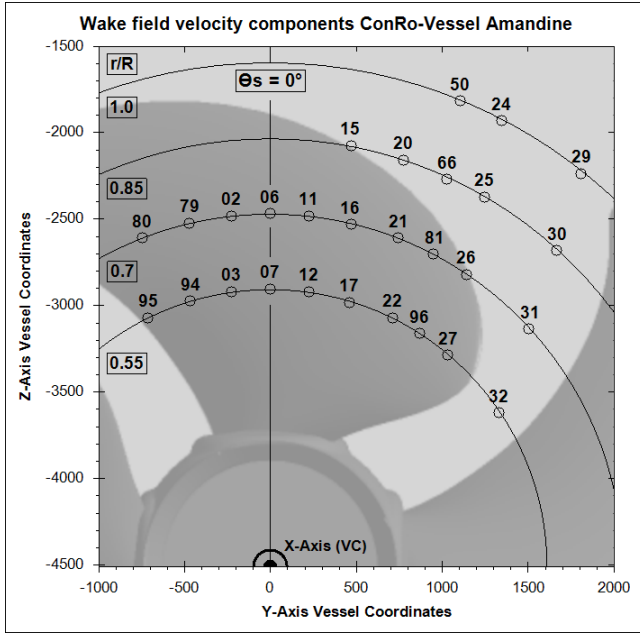


Figure 11: Coordinates of the measurement volumes, projected on the propeller plane.

A representative operating point (Table 4) for the ship was defined for the CFD calculation based on the analysis of the four measuring campaigns in the Irish Sea.

Table 4: Operation point for the numerical investigation.

Ship speed	V_S	[kn]	16.87
Draft	T	[m]	6.485
Dynamic sinkage	z_{VM}	[m]	0.1318
Trim angle	θ	[°]	0.0294
Number of revolutions	n	[rpm]	103.0
Propeller pitch ratio	$P_{0.7}/D$	[-]	0.9925

The calculation was accomplished using a RANS method simulating the flow around the underwater hull of the “Amandine” with the working propeller. The robust SST turbulence model, which assumes isotropic turbulence, has been applied. A block structured numerical mesh with approx. 7.2 million nodes was used. The extent of the computational domain was determined so that the flow around the ship is not influenced by the boundary conditions on the outer sides of the domain or blocking. The ANSYS software suite was used for the grid generation and the calculation. The ship is fixed in the computational domain and is flown to ship’s speed. The numerical calculation was performed for the ship in model and full-scale under consideration of the dynamic floating condition for the investigated operating point.

The local velocity components had been represented by the axial wake fraction w (1) where u is the local axial velocity and V is the speed of the ship.

$$w\left(\frac{r}{R}, \theta\right) = 1 - \frac{u\left(\frac{r}{R}, \theta\right)}{V} \quad (1)$$

Figure 12 shows the calculated distribution of the axial velocity components in the measurement plane for the respective angular position of the propeller.

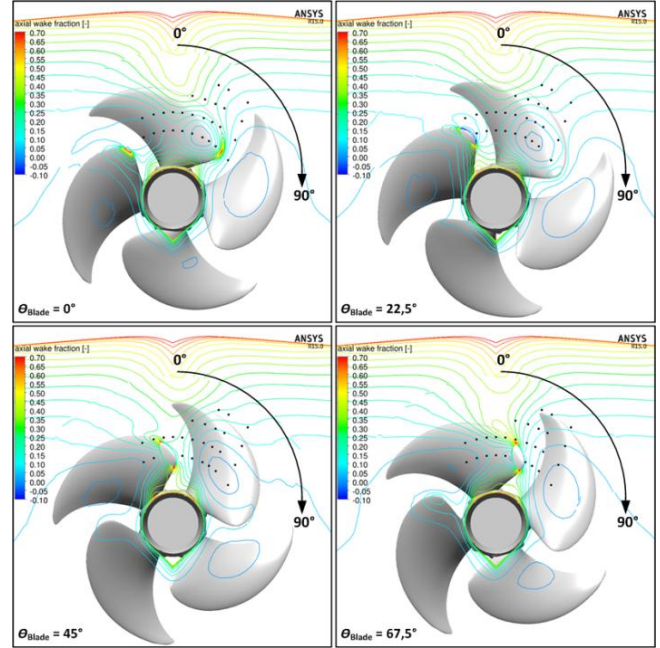
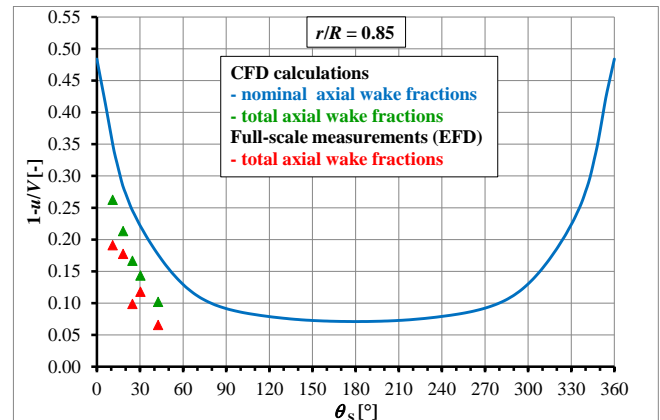


Figure 12: Calculated total axial wake fraction and visualization of measurement points (black dots) at the four angular propeller positions.

The diagrams in Figure 13 show the comparison of the calculated (green marks) and measured (red marks) total axial wake fractions in front of the propeller for the radii $r/R = 0.85$ and 1.00 . The velocity data were averaged over all propeller positions. An unfilled symbol indicates a missing value for one angular position, due to an intersection of the blade with the measurement plane. The black line represents the calculated nominal axial wake fraction without the working propeller.



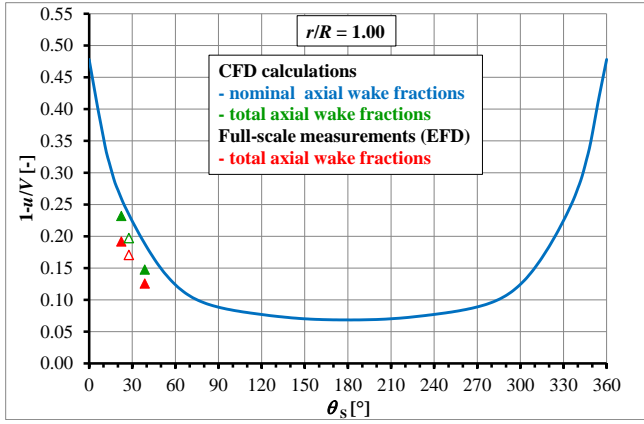


Figure 13: Comparison of calculated and measured total axial wake fractions (averaged over the four angular positions) with the nominal axial wake fractions.

The influence of the working propeller on the total wake is responsible for the higher velocities in comparison with the nominal wake. The comparison of the measured and calculated mean axial velocity components show small deviations of mostly less than 5%. But especially in the most interesting area for characterizing the width and deep of the wake peak (highlighted in red in Table 1) a systematic average deviation of almost 9% was revealed. This indicates average simulation inaccuracies. The real wake peak, characterized by lower velocities, is smaller than the calculated one.

Table 1: Differences between calculated and measured axial velocity components

$r/R = 0.55$		$r/R = 0.70$		$r/R = 0.85$		$r/R = 1.00$	
θ_s [°]	$\Delta u/V$ [%]						
333.5	-3.9	338.5	-1.3				
343.1	-2.7	346.6	-0.6				
351.8	0.7	353.6	-2.0				
0.0	0.9	0.0	1.9				
8.2	13.0	6.4	5.0	11.0	8.8	22.4	5.0
17.0	4.4	13.5	12.8	18.3	4.4	27.7	3.2
26.5	1.5	21.5	3.7	24.8	7.5	38.7	2.5
33.1	1.5	27.9	3.7	30.4	2.9		
40.5	3.5	34.3	3.7	42.6	3.9		
56.6	-1.7	47.9	4.9				

The velocity differences, listed in Table 1, are determined over formula 2.

$$\frac{\Delta \bar{u}}{V} = 1 - \frac{\left(\frac{\bar{u}}{\bar{V}}\right)_{CFD}}{\left(\frac{\bar{u}}{\bar{V}}\right)_{EFD}} \cdot 100\% \quad (2)$$

The diagrams in Figure 14 present examples of the calculated and measured variation of local axial velocities in front of the propeller, depicted over the four discrete propeller positions. The qualitative fluctuations of the total wake fractions are even in close proximity to the propeller

similar in the calculations and measurements. The quantitative differences are most significant at measuring points in the wake peak (MV16). With an increasing angular distance from the wake peak the deviation becomes smaller and more and more constant (MV21).

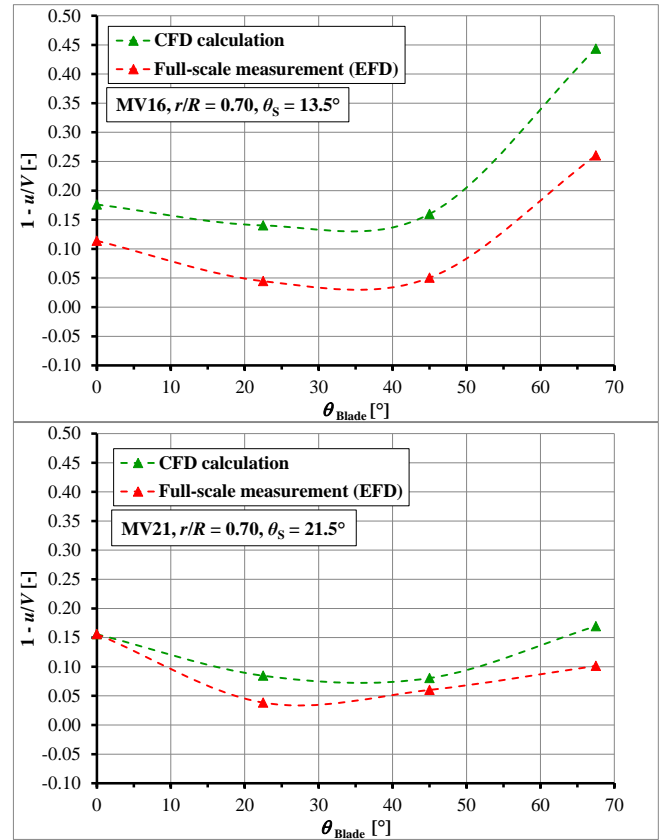


Figure 14: Comparison of the calculated and measured influence of the propeller blade position on total axial wake fractions at $r/R = 0.70$.

5 WAKE SIMULATION FOR MODEL TESTS

A dummy model and a propeller were built in a scale of $\lambda = 24.829$ for cavitation tests in the cavitation tunnel K15A of the SVA. The calculated nominal wake field for the ship at the full-scale Reynolds number (Figure 10 right) had been simulated by the dummy model and additional wire screens. The SVA is using the Laser-Doppler-Velocimeter (LDV) Innova 70 from TSI for carrying out wake velocity measurements during the simulation process.

The total velocity components in front of the model propeller could not measure in the same plane than at the ship due to limitations in the optical access. That's why it was decided to compare the velocity measurements at the dummy model with the CFD calculations in a parallel plane at a higher distance from the propeller, as shown in Figure 15.

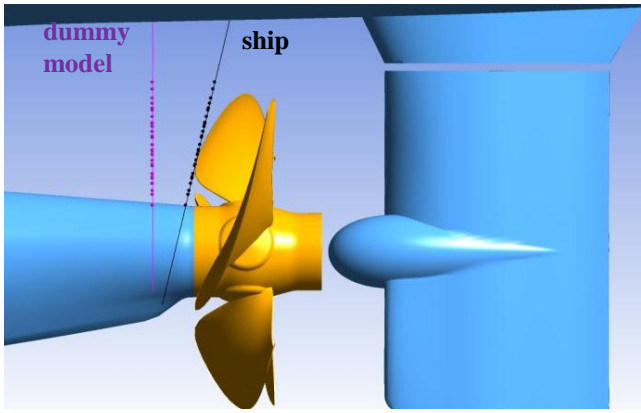


Figure 15: Measuring planes for total velocities at the dummy model and ship.

The effect of the working propeller on the total wake of the ship is distinctly smaller in the “dummy model plane” with a distance of $x/D = 0.2568$ from the propeller plane than in the “ship plane” very close to the propeller (Figure 16).

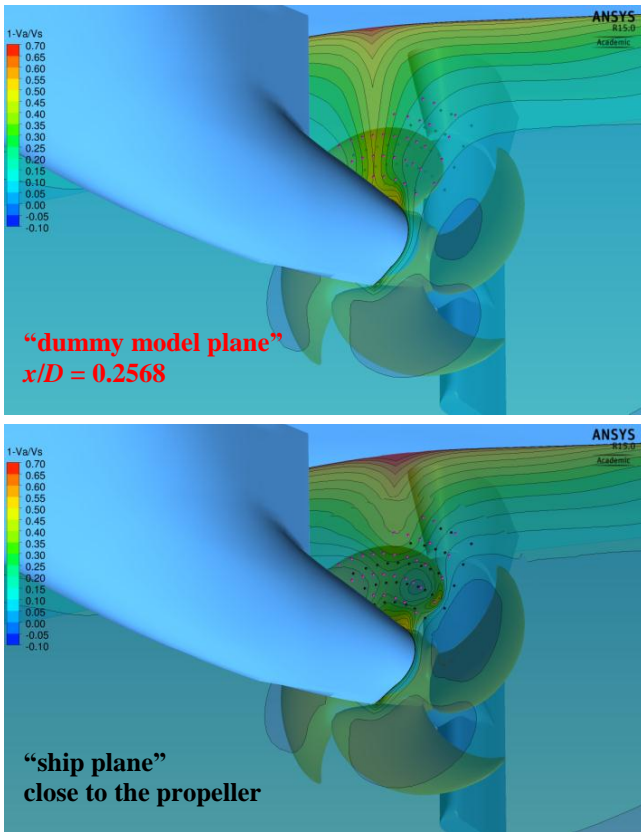


Figure 16: Changing of the total wake with the distance from the propeller, $\theta_{\text{blade}} = 0^\circ$.

The calculations of the total wake fractions for the ship had been used for a comparison with the nominal wake field in the propeller plane of the dummy model and LDV measurements at the dummy model with working propeller in the operation point for the cavitation tests.

The diagrams in Figure 17 show a good agreement between the measured total wake fractions at the dummy model and the calculated total wake fractions at the ConRo-ship “Amandine”. The maximum total wake fractions in the wake peak of the dummy model are mostly a little bit smaller than calculated for the full-scale.

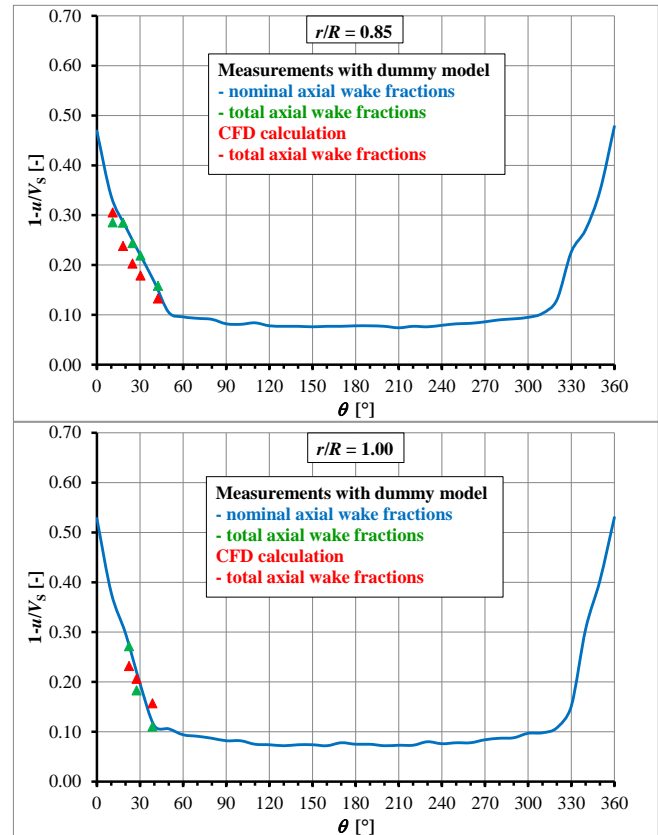


Figure 17: Comparison of nominal and total wake fractions at the dummy model with CFD calculations for the ship.

6 CAVITATION AND PRESSURE FLUCTUATIONS

The aim of the full-scale wake simulation for cavitation tests is the generation of a wake field, which represents as well as possible the propeller inflow situation as it is expected to be in reality (ITTC 2011). The result of the cavitation test is for example the cavitation behavior of the propeller, the inception of cavitation and the generation of pressure pulses. The results of a cavitation test can be influenced by test parameters (number of revolutions, water speed, pressure, nuclei content of the water, turbulence degree of the water) and other factors. That’s why the improvement in the simulation of a full-scale similar propeller inflow must not necessarily result in a better cavitation prognosis.

6.1 Cavitation Behavior of the Propeller

The observation of the propeller at the ConRo-ship “Amandine” showed tip vortex cavitation at the blades of the controllable pitch propeller, running with a constant propeller speed of 103 rpm (Figure 18).

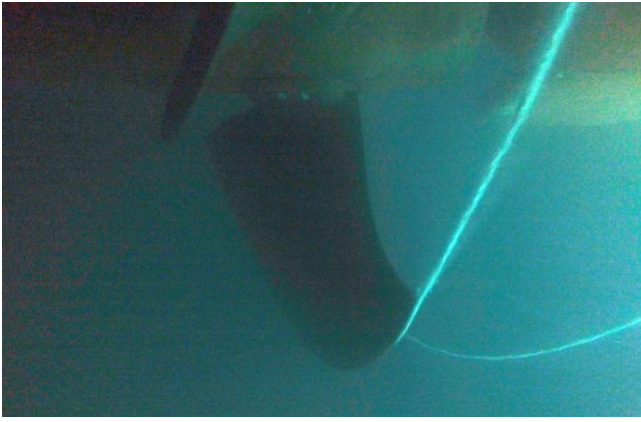


Figure 18: Tip vortex cavitation at the propeller of the ConRo-ship “Amandine”.

The cavitation tests with the dummy model in the cavitation tunnel K15A showed tip vortex cavitation at the model propeller which is not so strong developed than at the full-scale propeller (Figure 19). Also the CFD calculations show relatively weak developed tip vortex cavitation (Figure 20). These differences can be explained by the viscous tip vortex scale effect as treated by McCormick (1962).



Figure 19: Tip vortex cavitation on the model propeller in the operation point.

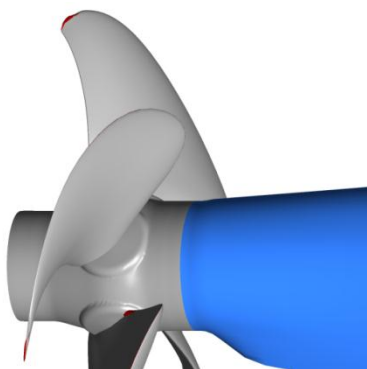


Figure 20: Cavitation prognosis for the operation point of the ConRo-ship “Amandine”.

6.2 Pressure Fluctuation Amplitudes

Full-scale pressure fluctuation measurements had been carried out aboard the ConRo-ship “Amandine” in August 2012 on a voyage from Rotterdam to Dublin and back, Weitendorf et al. (2013). The pressure fluctuation

amplitudes on the flat bottom above the propeller with a propeller tip clearance of abt. 30 % have been used for the comparison with the results of model tests and calculations in Figure 21. The blade harmonic pressure amplitudes from the cavitation test and the CFD calculation are mostly larger than the measured from the trial.

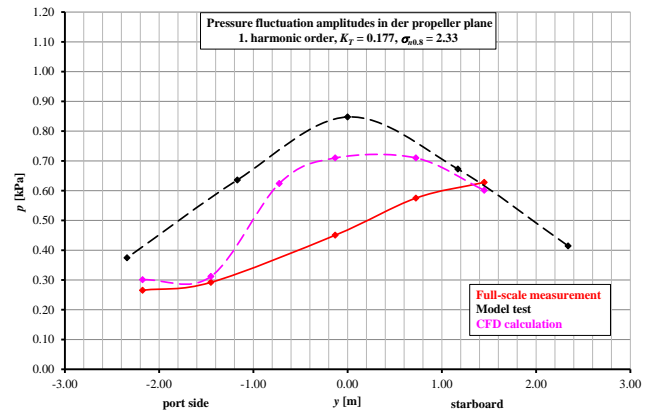


Figure 21: Blade harmonic pressure amplitudes in the propeller plane.

The smaller wake peak at the ConRo-ship “Amandine” in comparison with the CFD calculation (chapter 4.2) and in the cavitation test with the dummy model (chapter 5) can be one reason for the differences in the blade harmonic pressure fluctuation amplitudes, measured aboard and calculated or measured in the cavitation test.

7 CONCLUSIONS

The novel PIV-technique is well suited to record wake field velocity data at full-scale. A high statistical secure data rate, a wide angular range in front of the propeller, a robust setup and a precise definition of the measurement volumes allow reliable measurements and offer great opportunities for further wake field investigations.

Full-scale total wake measurements in front of the controllable pitch propeller of the ConRo-ship “Amandine” had been used for the validation of viscous flow calculations for the ship with working propeller. In general there is a good agreement between the measured and calculated total velocity components. But especially in the wake peak are major discrepancies with the tendency that the real inflow speed in the wake peak is larger than calculated. The lower level of the propeller induced pressure fluctuation amplitudes in the first harmonic order in the trials in comparison with cavitation tests and calculations could be a result of the differences in the wake peak.

The scale effect on the propeller inflow has been confirmed by the analysis of the full-scale total wake measurements and CFD-calculations for the full-scale Reynolds number.

The measuring plane for the total wake measurements was too close to the propeller due to the given arrangement of

the portholes in the propeller plane. Further investigations should be carried out in a plane clearly in front of the propeller. The measurements close to the propeller complicate the evaluation of the measured velocities due to their high sensitivity against uncertainties like small changes in the propeller pitch and number of revolutions.

8 ACKNOWLEDGMENT

The authors would like to express their gratitude to the Federal Ministry for Economic Affairs and Energy for funding the project KonKavII (grant number 03SX316D). Many thanks are addressed to the partners in the R&D-project for the excellent co-operation and their support in the preparation and analyses of the full-scale measurements. The responsibility for the content of this publication lies with the authors.

REFERENCES

- Carlton, J. (2012) Marine Propellers and Propulsion, Elsevier Ltd.
- ITTC (1999). The Specialist Committee on Computational Method for Propeller Cavitation, Proceedings of the 22th ITTC, Seoul and Shanghai.
- ITTC (2011). The Specialist Committee on Scaling of Wake Field, Proceedings of the 26th ITTC – Volume II, Rio de Janeiro.
- Kleinwächter, A., Ebert, E., Kostbade, R., Hellwig-Rieck, K., Heinke, H.-J., Damaschke, N. A. (2014). “Full-Scale Total Wake Field PIV-Measurements for an Enhanced Cavitation Prediction”, 17th Symposium on Applications of Laser Technologies to Fluid Dynamics, Lisbon.
- Kuiper, G., Grimm, M., McNeice, B., Noble, D., Krikke, M. (2002) Propeller Inflow at Full Scale During a Manoeuvre, 24th Symposium on Naval Hydrodynamics, Fukuoka.
- Kux, J., Niemeier, T., Stöhrmann, H. (1982). “LDV Wake Measurements Onboard Sydney Express”, Report No. 424, Shipbuilding Institute, University of Hamburg (in German).
- McCormick, J. (1962). "On Cavitation produced by a Vortex trailing from a Lifting Surface", ASME J. Basic Eng.
- Raffel, M., Willert, C. E., Wereley, S. T., Kompenhans, J. (2007). “Particle Image Velocimetry”, Springer-Verlag.
- Weitendorf, E.-A., Lücke, T., Richter, H., Schiller, P. (2013). “Nuclei and Cavitation Induced Pressure Fluctuations – Investigations in Two Cavitation Tunnels and Full Scale”, STG-Colloquium “Advanced Experimental and Computational Methods for Investigation of Cavitating Flows”, Hamburg.